 doi:10.20944/preprints202011.0483.v1

Article

Optimization of thin walls with sharp corners in SS316L and IN718 alloys manufactured with laser metal deposition

Juan Carlos Pereira [1,*], Herman Borokov [1,2], Fidel Zubiri [1], Mari Carmen Guerra [3] and Josu Caminos [4]

[1] LORTEK Technological Centre, Basque Research and Technology Alliance (BRTA), Arranomendia kalea 4A, Ordizia (Gipuzkoa), Spain; jcpereira@lortek.es
[2] Faculty of Engineering, University of Deusto, Avenida de las Universidades 24, Bilbao (Vizcaya), 48007, Spain; hborovkov@lortek.es
[3] Aotek S. Coop., San Andrés 19, Arrasate-Mondragon (Gipuzkoa), Spain; mcguerra@aotek.es
[4] FAGOR Automation S. Coop., San Andrés 19, Arrasate-Mondragon (Gipuzkoa), Spain; jcaminos@fagorautomation.es
* Correspondence: jcpereira@lortek.es; Tel.: +34 943882303

Abstract: In this work, the manufacture of thin walls with sharp corners has been optimized by adjusting the limits of a 3-axis cartesian kinematics through data recorded and analyzed off-line, such as axis speed, acceleration and the positioning of the X and Y axes. The study was carried out with two powder materials (SS316L and IN718) using the directed energy deposition process with laser. 1 mm thick walls were obtained with only one bead per layer and straight/sharp corners at 90°. After adjusting the in-position parameter G502 for positioning precision on the FAGOR 8070 CNC system, it has been possible to obtain walls with minimal accumulation of material in the corner, and with practically constant layer thickness and height, with a radii of internal curvature between 0.11 and 0.24 mm for two different precision configuration. The best results have been obtained by identifying the correct balance between the decrease in programmed speed and the precision in the positioning to reach the point defined as wall corner, with speed reductions of 29% for a programmed speed of 20 mm/s and 61% for a speed of 40 mm/s. The walls show minimal defects such as residual porosities, and the microstructure is adequate.

Keywords: additive manufacturing; laser metal deposition; thin walls; sharp corner; cartesian kinematic; FAGOR 8070 CNC

1. Introduction

In Additive Manufacturing (AM) using Directed Energy Deposition (DED) process like Laser Metal Deposition (LMD) it is necessary to keep the process stable in terms of the deposition rate, layer height, and powder efficiency, to avoid imperfections and accumulation of deposited material in certain areas, so it is necessary to adjust process parameters, the drives and the kinematic itself, as well as the powder feeding/delivery system. Optimizing the process for small laser spot and thin walls is a challenge. In this adjustment process, the use of the recorded data via OPC-UA and its interpretation are of utmost importance to achieve the stability of the deposition process and to correct potential defects.

According to ISO/ASTM 52900 standard [1], DED is the AM process in which focused thermal energy is used to fuse materials by melting as they are being deposited. "Focused thermal energy" means that an energy source (for example: laser, electron beam, or plasma arc) is focused to melt the materials being deposited. Under this definition, LMD is considered a laser-based DED process (LB-DED) that use a laser beam as a thermal energy source to melt the material. More in detail, the ASTM F3187 standard [2] details the composition of DED systems, which are made up of four fundamental

Preprints (www.preprints.org) | NOT PEER-REVIEWED | Posted: 18 November 2020 doi:10.20944/preprints202011.0483.v1

subcomponents: heat source, positioner (motion), feedstock feed mechanism, and a computer control system. In the case of LMD system, the motion is achieved either by moving the heat source relative to a stationary component, or moving the component relative to a stationary heat source, or a combination of these methods. Motion is typically provided in at least three orthogonal axes. Integrated motion of auxiliary axes (rotary, tilt axes), working with the main motion control axis (Cartesian gantry or 6-axis robotic arm), are typically used. In LMD systems the laser beam is conducted from the laser source to the optic head through optical fiber, and the material to be supplied is delivered by a nozzle, which can be coaxial to the beam (assembled to the optic head) or deliver the material laterally. Feedstock material can be used in this process in the form of wire or powder. Figure 1 shows the coaxial LMD-powder process with powder as used in this work, where the nozzle, laser beam, powder stream and melt pool formation can be observed.

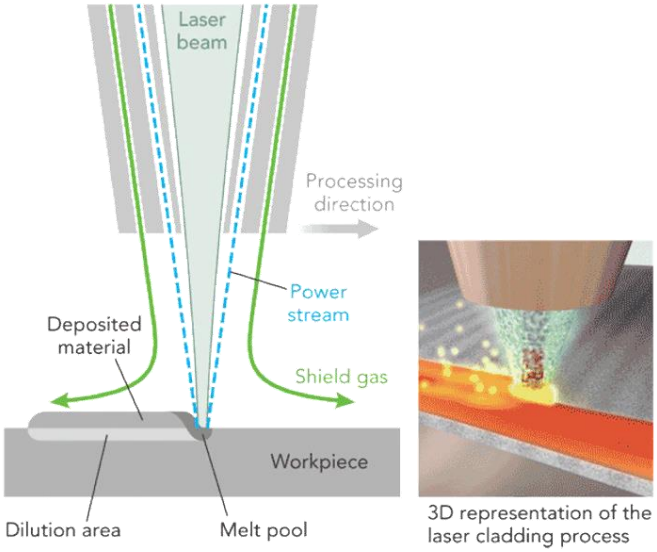

Figure 1. Schematic representation of coaxial LMD process with powder (LMD-p)[3].

In the Laser Metal Deposition (LMD) process, the adjustment of the kinematics is of utmost importance in order to manufacture thin walls with abrupt changes in trajectories, as occurs in thin walls with straight corners. For the kinematic adjustment and the parameters of the deposition process it is of utmost importance to be able to monitor data from variables such as axis velocity, axis acceleration, nozzle position, size of the melt-pool, layer height, etc., and analyze them in depth to develop LMD process new optimization strategies or to apply machine learning.

Previous studies investigated the effect of the process parameters like laser power, spot diameter, scanning speed (velocity) and powder feed rate on the DED process. The influence of the main LMD process parameters on the bead geometry is well known and extensively reported for different metallic materials. Zhang *et al.*[4] carried out comprehensive experiments on the laser metal deposition process with nickel-based superalloy to investigate the effect of these process parameters on the forming shapes via additive manufacturing. Davim *et al.* [5] evaluated the effect of the process parameters including laser power, scanning velocity, and powder mass flow rate on the geometric form of a cladding. They showed that the cladding height increases with the powder mass rate and the laser power and decreases with the velocity. The penetration depth increases with the laser power and the powder mass flow rate. The cladding width increases with the powder mass flow rate. In particular for the deposition of IN718 alloy, Zhong *et al.* [6] showed some metallographic properties regarding material defects, especially porosity, as well as microstructures such as grain orientations, elements segregations and phase precipitations of the as deposited material. Confirming the complexity of laser processing for this material and the necessity of post-processing like hot isostatic pressing (HIP) and a solution plus double aging heat treatment to improve the mechanical properties.

Conventional scanning paths for computer numerically controlled (CNC) systems (like in Cartesian kinematics) are mainly composed of linear motion segments. The scanning speed of the conventional system is decreased near the junction point to change the direction of the scan track.

Preprints (www.preprints.org) | NOT PEER-REVIEWED | Posted: 18 November 2020 doi:10.20944/preprints202011.0483.v1

This change may lead to serious limitations in terms of achieving the desired part of geometry and productivity by over depositing near the corner section because velocity and acceleration discontinuities occur at the junction points of consecutive segments. Over deposition can cause loss of geometric tolerance requiring post processing to obtain geometric accuracy. Some authors published interesting results developing algorithms to control the scanning-speed to generate smooth and equal-height deposition, in geometries with walls and corners [7]. Therefore, the control method enabling the DED fabrication of an equal-height rectangular acting over bead geometry measured or predicted but only take into consideration the layer height and not the precision of the wall thickness or internal/external radii in the wall´s corner.

Others author tried to solve this problem of material accumulation during the deposition with the implementation of a closed-loop control acting on the laser power [8] but the time response of this strategy is too high to correct the problem in corners of thin walls in real time [9,10]. And also the measuring of layer height and control procedure based on structured light scanning has been set up in an LMD robotic cell. The benefit of measuring and controlling the build height during the process was proved [11], showing a more accurate reproduction of the generated geometry in solid parts when corrections are applied, but this approach need to stop the deposition process to scan and generate a three-dimensional point cloud, that requires to be processed by previously developed algorithms, which is time-consuming process and add extra time to the additive manufacturing stage.

In Cartesian kinematics, one option is to adjust the deposition rate and the acceleration/deceleration on the axes, which has a large influence on the deposition rate but also on the positioning [12–14]. This tuning of the algorithm has been optimized thanks to FAGOR Datalogger which can register valuable data on a millisecond scale time basis. It is also capable of executing real-time data filtering in order to avoid false positives by sampling signals and applying digital IIR filters. Results obtained with this tool are useful to improve the movement of the axes while material deposition is executed. The performance of the machine can be monitored remotely by using OPC-UA, an industrial communication protocol which delivers data from machine to end user on a classic client-server architecture [15]. This technology is widely used on industrial environments all over the world due to its openness, in-built security, scalability and information modelling. It can be considered the standard of industry 4.0 and has been the underlying technology to retrieve data from the CNC.

In this work, we have studied how to use the monitored and recorded data in a 4-axis Cartesian kinematic station with a CNC FAGOR 8070 arranged for LMD process in LORTEK. In particular, the velocity and acceleration in each axis to generate deposition strategies in 2.5D that correct the problems that currently arise when the deposition trajectory is discontinuous using constant process parameters, that is, where there are abrupt changes of direction or in sharp corners for example. The discontinuous deposition in these trajectories causes uneven deposition, leading to problems of material accumulation, variation in layer height and in some cases defects like lack of fusion and porosity in singular points/zones.

2. Materials and Methods

In this work two different alloys were used, an austenitic stainless steel (316L) and a Nickel-based alloy (IN718). The gas atomized powders manufactured by TLS Technik GmbH & Co. Spezialpulver KG (Bitterfeld-Wolfen, Germany) have the same particles size in terms of granulometry, 45-90 µm according their specifications. The chemical composition reported by the manufacturer is showed in Table 1.

Table 1. Chemical composition of SS316L and IN718 powders used in LMD process (measured by TLS Technik).

Alloy	Elements and Chemical Composition range (wt.%)											
	C	Mn	Si	Cr	Ni	Mo	Nb	Ti	Co	Al	Fe	Others
SS316L	0.020	1.10	0.60	16.90	11.8	2.30	---	---	---	---	Bal.	---
IN718	0.024	0.09	0.07	17.68	54.2	2.95	5.17	0.96	0.28	0.47	18.02	0.085

Preprints (www.preprints.org) | NOT PEER-REVIEWED | Posted: 18 November 2020 doi:10.20944/preprints202011.0483.v1

The pre-alloyed powders used in this work for the LMD samples showed a spherical morphology (Figure 2 left), typical of the gas atomization process. After size analysis of the particles, the results revealed that a cumulative 10% in volume of the particles had a diameter of less than 36.5 and 70.6 microns for SS316L and IN718 powders; 50% of the particles had a diameter of less than 51.1 and 81.8 microns; and a cumulative 90% volume of the powder particles had a diameter of less than 79.9 and 91.1 microns respectively. The analysis of particle shape and size distribution (diameter) in the powder shown in Figure 2 (right) is very important for the LMD process. As can be seen, the particle size distribution for IN718 is more closed and with less range of variability than those of SS316L, a greater quantity of fine or smaller diameter particles is observed in the SS316L powder. Due to the typical powder feeder system used in directed energy deposition (DED) process, a fine-medium granulometry and regular sizes and shapes are required, and an adequate flowability of the powder determines the best powder stream in the coaxial nozzle for laser melting and deposition of the raw material.

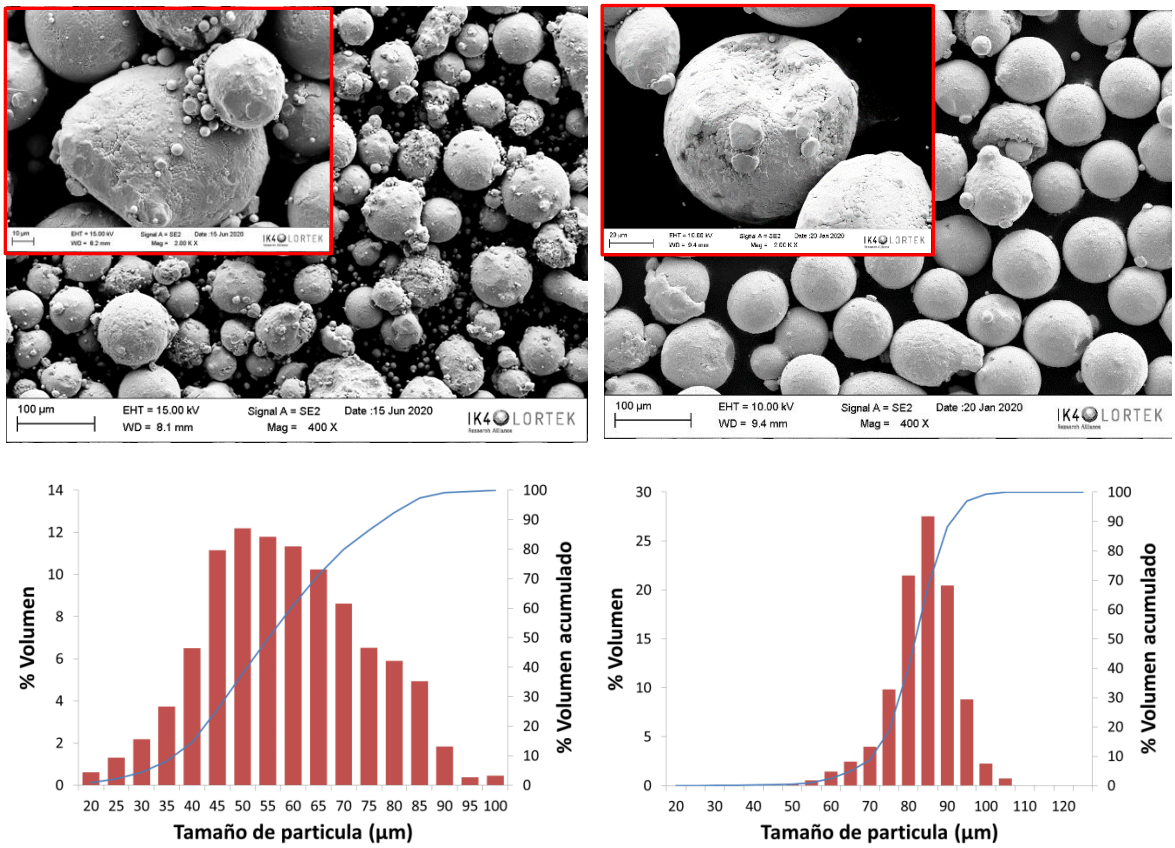

Figure 2. Characterization of pre-alloyed gas atomized powders. Morphology of the particles in SEM image (20 kV), and Granulometry and distribution analysis. SS316L powder (left) and IN718 Powder (right).

The LB-DED system used for the LMD process was a 3-axis Cartesian kinematic station equipped with classical CNC (FAGOR 8070, Spain), see Figure 3 (left), and a solid state laser source Nd-YAG of 3kW (Trumpf HL-3006D, Germany) in CW mode and wavelength 1.06 µm with a spot diameter of 1.2 mm. The configuration of the LMD station include an optic head (Trumpf BEO D70, Germany) with two on-axis camera/sensor ports. For powder delivery, the LMD station has a powder feeder with two heated hoppers (Sulzer-Metco Twin-10C, Switzerland) and a coaxial nozzle (Coax40, manufactured by FhG ILT, Germany) was used (Figure 3 right). Argon was used as protective (8 L/min) and carrier gas (flow at 1 bar).

Preprints (www.preprints.org) | NOT PEER-REVIEWED | Posted: 18 November 2020 doi:10.20944/preprints202011.0483.v1

Figure 2. Cartesian kinematics LMD station in LORTEK. Detail of the station (left) and detail of the Coax40 nozzle with the powder flow (right).

The optimized LMD process parameters for each material are compiled in Table 2.

Table 2. LMD process parameters for the manufacturing of thin walls.

Material	Power (W)	Laser spot diameter (mm)	Velocity (mm/min)	Mass flow (g/min)	Energy (J/mm2)	Layer thickness (mm)
SS316L	400	1.2	500	3.9	40	0.5
IN718	400	1.2	500	5.0	40	0.5

For microstructural evaluation, the samples were cut from walls manufactured over SS304 stainless steel plates of 10 mm thickness, and conventional metallographic preparations were made. The metallographic preparation procedure followed the guidelines of ASTM E3 standard [16], embedding the samples in resin to then carry out a roughing with abrasive papers with different granulometry, and a final polishing with diamond particles in suspension. For the chemical etching, the reagents recommended for each material in the ASTM E407 standard [17] have been used. The macro and microstructural analysis was carried out using an optical microscope (OM) with an Olympus GX51 optical microscope with an image acquisition system via digital camera. Manual chemical etching was carried out with Nital at 5% for 12s. The micrographs were evaluated at different magnifications (100X, 200X and 500X). For advanced microstructural evaluation, a Zeiss Ultra Plus FESEM microscope equipped with X-Max Oxford Instruments system and x-ray silicon drift detector (SDD) of 20 mm^2 was used, to perform semi-quantitative analysis of the chemical composition by energy dispersive spectroscopy (EDS). Microhardness Vickers measurements were made in an EmcoTest DuraScan durometer, using a load of 500 grams (HV0.5 scale).

3. Results and their analysis

The initial work has been to analyze the data acquired through the platform previously developed by FAGOR Aotek and LORTEK for data acquisition and remote connectivity of the LMD

Preprints (www.preprints.org) | NOT PEER-REVIEWED | Posted: 18 November 2020 doi:10.20944/preprints202011.0483.v1

station. We have started with the definition of a series of experimental tests to evaluate the influence of trajectory programming and speed/acceleration control on the quality of deposition on a straight trajectory but with a 90° corner.

Taking advantage of the algorithms integrated in FAGOR CNC systems, it is possible to tune the movements of the axes in the machine to avoid problems related to material accumulation in corners and achieve accurate geometries in an effective way. FAGOR provides by default several subroutines, so end users can configure dynamically the motion of the machine. G502 is an example of these in-built subroutines. One of the inputs to this procedure is parameter "e", which stands for tolerance in millimeters between the points defined in part programs and the real trajectory performed by the axes. FAGOR CNC system commands the axes, so the distance between programmed position and real trajectory never exceeds the configured tolerance. Theoretically, higher tolerances make the dynamic of the machine more fluid and smooth, achieving more homogeneous material deposition in corners.

Datalogger can filter and register data on a millisecond scale time basis. Several variables are recorded simultaneously, such as axes trajectory, speed, acceleration, nominal laser power... All of them can be real-time filtered individually, so unnecessary data can be removed from results. This data can be exploited remotely thanks to an industrial communication protocol compatible with FAGOR systems: OPC-UA. This technology enables a secure delivery of data between remote servers and clients, stablishing a bidirectional communication between them. While the state of the machine and its components can be monitored remotely on HTML5 webpages, data is also recorded on files, so historical statistics can be obtained through deep offline analysis of these files. As a result of these exhaustive calculations, the movement of the axes is optimized to get the correct deposition rate in every circumstance.

Using the data acquired from the CNC 3D plots of real coordinates and speed variation can be elaborated. Such approach allows an operator to monitor the process parameters and detect possible failures with 4 ms time resolution. Apart from that, the deep data analysis in both time and layer/distance domains is extremely valuable. Also, 3D analysis, acquisition and synchronization of the CNC kinematics data is a part of a platform for "digital twin" which will include data from both CNC and external process sensors.

To demonstrate the analysis methodology, thin corner walls have been manufactured as semi-complex geometry demonstrators, in AISI 316L stainless steel and IN718 nickel base alloy. The thin walls are approximately 1.20mm thick and have 50 layers for a total height of 25 mm (see Figure 4).

Figure 4. Thin walls manufactured by LMD-powder. 20x40x25 mm wall made of SS316L without process control (left) and 30x50x10 mm wall made of IN718 with process control (right).

3.1. Kinematic precision analysis

The objective here has been to analyze how the corner point is reached with the highest possible accuracy (lower d in Figure 5), keeping the deposition rate with the least possible variation (lower %Vred). In the Cartesian CNC station, the programming parameter G502 e:X.XX related to the

Preprints (www.preprints.org) | NOT PEER-REVIEWED | Posted: 18 November 2020 doi:10.20944/preprints202011.0483.v1

positioning accuracy must be adjusted, according to models or initially according to the experimental analysis. In this case its influence has been analyzed for two different programmed speeds without deposition (only kinematic movement) and recording the position, real speed and real acceleration data in each axis.

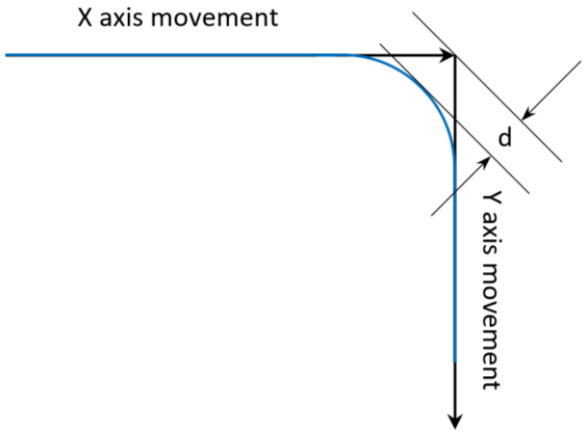

Figure 5. Deviation of the deposition path when approaching a straight corner in the LMD process.

Different variables have been recorded at the LMD station through the datalogger developed by FAGOR. Three variables are of interest for this study: the speed (Speed parameter measured, Vreal) and the position in each axis (Coordinates parameters measured: PosX and PosY) as a function of time for each combination of precision in positioning. The data acquisition parameters have been following:

- Measurement step (s): 8ms
- Programmed speed (v): 20 and 40 mm/s
- Precision (e): 0.04, 0.1, 0.4 y 0.6 (programmed through FAGOR in-position code G502 e:x.xx)

Figure 6 shows the registration of the positioning in the two axes (X and Y) in the proximity of the corner (programmed path for a wall in L) for the two speeds studied, using point to point programming through a linear interpolation (G01) between them. It is verified as the increase in the accuracy of the reach of the point defined as corner, the greater the distance of the path to it and therefore greater rounding will present the path at the corner.

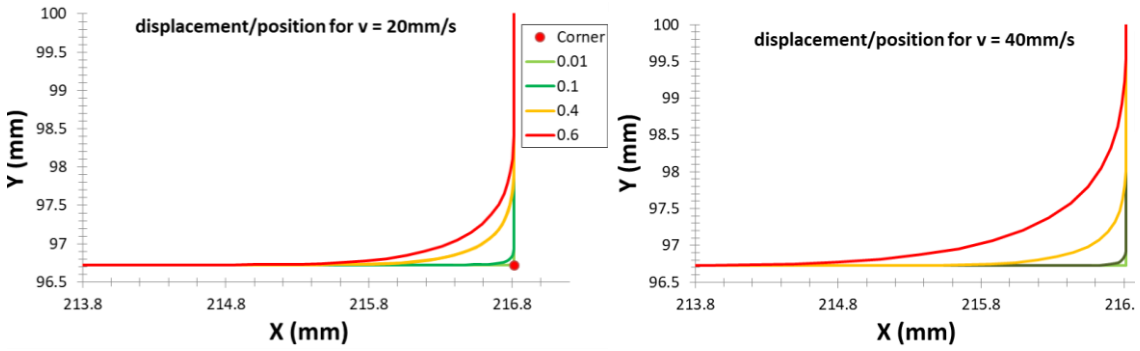

Figure 6. Position register (X and Y axes) in the vicinity of the corner for different values of e: X.XX and two speeds (v = 20 mm/s and v = 40 mm/s).

On the other hand the speed also decreases with respect to the programmed or theoretical for greater accuracy, and it is possible to determine how much this variation is in percentage terms and also know for high speeds when the speed control begins to act (kinematic correction) and in what proximity to the corner it does. This allows, taking the considerations intrinsic to the process of DML

Preprints (www.preprints.org) | NOT PEER-REVIEWED | Posted: 18 November 2020 doi:10.20944/preprints202011.0483.v1

define and adjust the accuracy for a given geometry involving changes in direction or sharp corners without circular interpolation. The speed control on the motors that move the table in the X and Y axes in FAGOR stations is considered adequate, the registration of actual speed has little variation. After graphical analysis of the speed behavior, it has been calculated the percentage reduction of speed for each accuracy and compared the results for the two speeds under study, also determining the reaction time during speed correction for each accuracy. In Figure 7 you can see in more detail how the speed variation occurs in the proximity of the corner. The velocity variation in linear and away from the corner or start/end of the trajectory is stable with no appreciable variation.

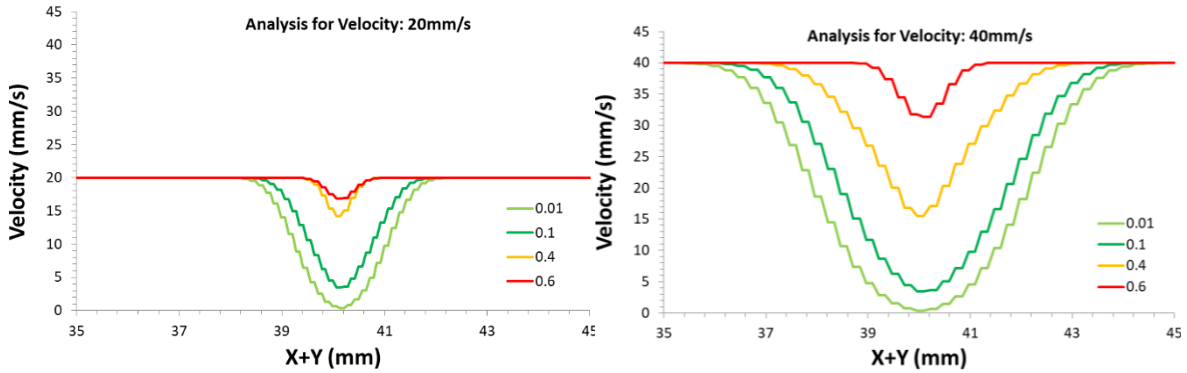

Figure 7. Speed recording as a function of position on each axis in the vicinity of the corner. v = 20 mm/s (left) and v=40 mm/s (right).

By performing the corresponding calculations to obtain the parameter "d" defined as the distance of the curvature from the programmed corner point (or change of direction, see Figure 5), and by calculating the speed drop in percentage terms as well as the reaction time during the speed adjustment, it is possible to analyze the kinematics accuracy. Table 3 shows the calculated values for the FAGOR LMD station on LORTEK.

Table 3. Results obtained with Cartesian kinematics and FAGOR CNC 8070 in LORTEK facilities.

Velocity	Precision, e:X.XX (Adim)	d (mm)	Vred (%)	Reaction time (s)
20 mm/s	0.01	0.044	97.99	0.23
	0.10	0.164	82.75	0.19
	0.40	0.429	28.83	0.12
	0.60	0.764	15.90	0.11
40 mm/s	0.01	0.020	98.97	0.25
	0.10	0.307	91.46	0.22
	0.40	0.975	61.25	0.19
	0.60	1.942	21.60	0.12

Finally, it has been analyzed through 3D plots the speed variation in two successive layers (Z1 and Z1+0.5mm), programming linear trajectories (G01) for trajectories of a wall that would be manufactured with a single cord. As commented before, the speed variation is the same in each layer, the variation of the Z coordinate has not been registered, and the deceleration at the end of linear paths is also observed, similar to what happens in the vicinity of a corner or in a sudden change of direction. The results are shown below in the graphs in Figure 8 and Figure 9 for both speeds and two of the accuracies studied (e:0.01 and e:0.40).

Preprints (www.preprints.org) | NOT PEER-REVIEWED | Posted: 18 November 2020 doi:10.20944/preprints202011.0483.v1

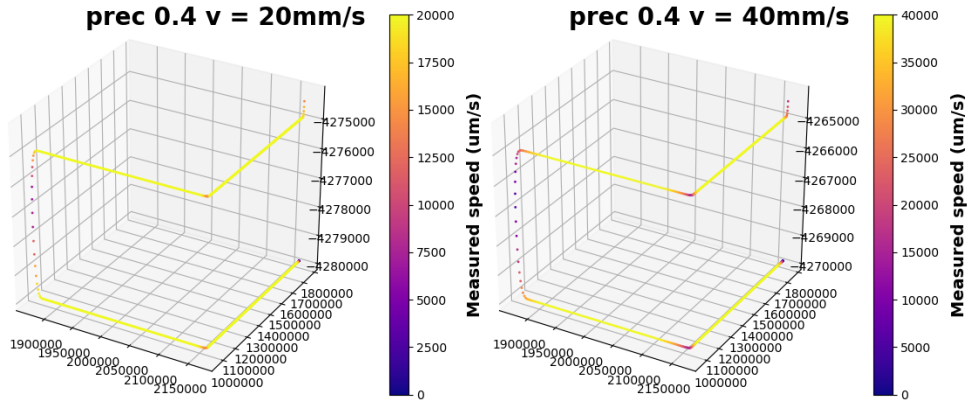

Figure 8. 3D plot of position as a function of velocity (precision e = 0.4) for two successive layers

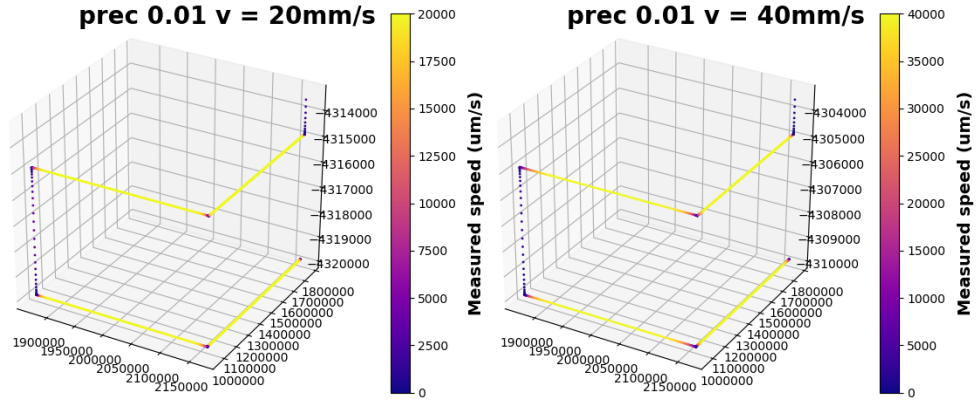

Figure 9. 3D plot of position as a function of velocity (precision e = 0.4) for two successive layers.

3.2 Geometric precision of thin walls with sharp corners

In order to evaluate the influence of the e:X.XX parameter and the use or not of the laser power control system during the deposition process, thin walls (thickness 1.20 mm and one bead per layer) have been manufactured with different materials, then we have proceeded to analyze through optical microscopy and micrograph processing by image analysis the curvature (internal and external radius) and quality of the material. For demonstration purposes, the walls have been manufactured with lower speeds than those used in kinematics analysis. The process parameters are compiled in Table 2. It can be seen in Figure 10 that the best results are achieved with e=0.40 for a speed of 500 mm/min with or without power control, since the phenomenon of material build-up that occurs when the kinematics are adjusted with greater positioning accuracy (e=0.04 and 500 mm/min) is minimized. The measured values of the radius of curvature both internally and externally at the corner of the manufactured walls are compiled in Table 4.

Preprints (www.preprints.org) | NOT PEER-REVIEWED | Posted: 18 November 2020 doi:10.20944/preprints202011.0483.v1

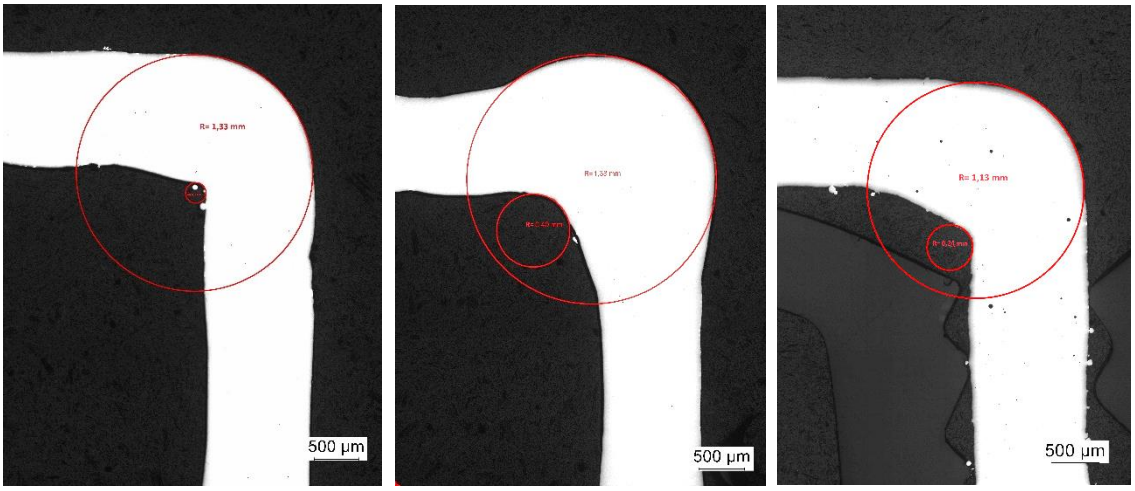

Figure 10. Radius of curvature in thin walls made with powder LMD. SS316L walls without power control, with e = 0.40 (left), e = 0.04 (center) and wall in IN718 with e = 0.40 and power control (right).

Table 4. Measured inner and outer radius values

Sample	Material	Parameter G502 e:X.XX	Laser power control	Inner radius (mm)	Outer radius (mm)	Mean radius (mm)
1	SS316L	0.40	No	0.11	1.33	0.72
2	SS316L	0.04	No	0.40	1.38	0.89
3	IN718	0.40	Yes	0.24	1.13	0.69

This tendency to accumulate material right in the corner, and the reduction of wall thickness before and after the corner, is more evident in sample 2 manufactured with SS316L, where the power control system has not been worked with and where the lowest value for the kinematics precision parameter has been used, in turn in this sample the greatest speed reduction has been registered in the vicinity of the corner.

3.3 Microstructure and mechanical properties

In this section, the microstructure and mechanical properties in the walls obtained with both study materials obtained through direct deposition processes (LB-DED) and with the geometries specified above have been evaluated. It has been cut the cross section of the walls manufactured in the area near the corner, and it has been studied from the anchorage of the filler material with the substrate material, as well as the wall at two different heights, towards 5 mm in height and towards 10 mm in height.

A first analysis of possible defects present in the cross section of the wall has been carried out for the different samples in a polished condition without attack. In Figure 11, it can be seen that the walls made of SS 316L (samples 1 and 2) do not show any lack of fusion or porosity, so it can be stated that the process parameters and energy density (40 J/mm^2) used in these stainless steel samples are adequate. In the case of sample 3 manufactured in IN718, no lack of fusion are observed, but small circular pores are observed, perhaps due to trapped gas from the used powder (gas atomized) or due to the use of excessive laser energy density (40 J/mm^2) since this material has a lower fusion temperature (1336 °C) than 316L stainless steel (1400 °C) and may require less energy for melt in LMD process. This leads to the conclusion that the process parameters need to be further optimized specifically for this material.

Preprints (www.preprints.org) | NOT PEER-REVIEWED | Posted: 18 November 2020 doi:10.20944/preprints202011.0483.v1

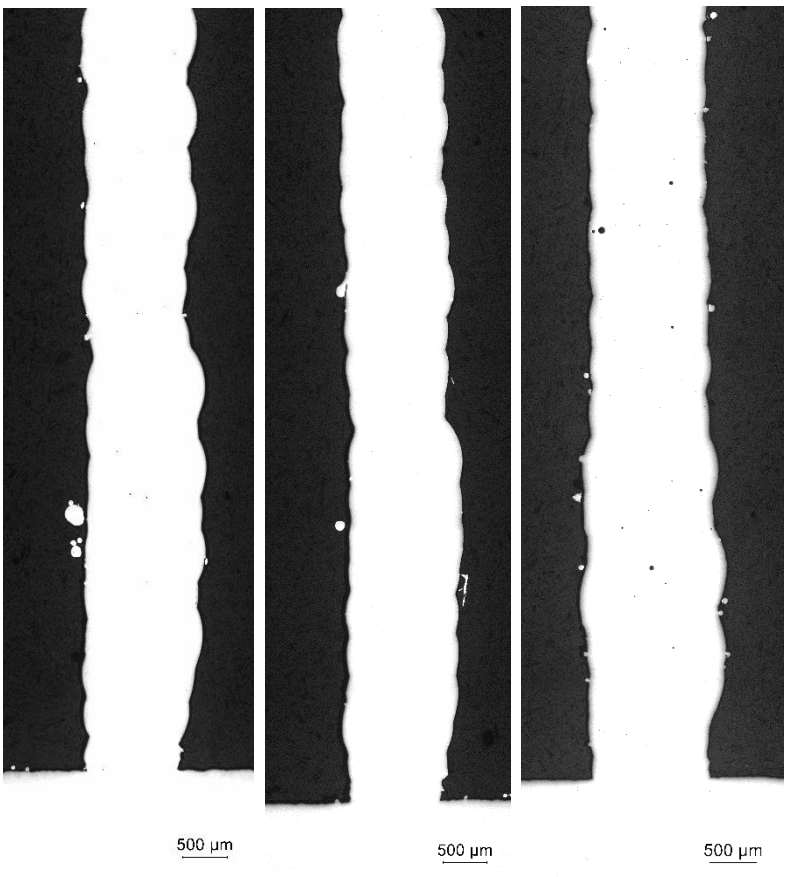

Figure 11. Photomicrograph of walls in a polished state. SS316L walls of sample 1 (left), sample 2 (center) and sample 3 wall manufactured with IN718 (right).

Once the samples have been chemical etched, it is now possible to analyze the microstructure of each sample and material used. Figure 12 (left) shows three different zones on the wall of the sample 1. At the interface with the substrate, the dilution zone with the base material (SS AISI 304) and the good metallurgical bond between both can be clearly seen. Also in this zone the mechanism of solidification of the first deposited bead is evident, where the microstructure is a very fine cellular dendritic structure. In the micrograph of the middle zone of the wall, it is already observed a columnar dendritic microstructure with epitaxial growth where changes in the direction of growth of the dendrites in the interface between cords are evidenced. In this middle zone the composition looks uniform without an apparent segregation. This microstructure is similar to that reported by other authors [18]. Furthermore, it can be deduced that the microstructure is composed of a matrix of γ austenite (light phase) and possible formation of ferrite in the cells (dark phase). The ferrite content is much lower than that of austenite as observed.

In sample 2 the microstructures of the three zones under study (Figure 12 right) is similar to that observed in sample 1, perhaps a smaller size of the dendrites is observed so that a smaller amount of ferrite (dark phase) is presumed, however, it may also be influenced by a less severe chemical etch than for the other sample.

Preprints (www.preprints.org) | NOT PEER-REVIEWED | Posted: 18 November 2020 doi:10.20944/preprints202011.0483.v1

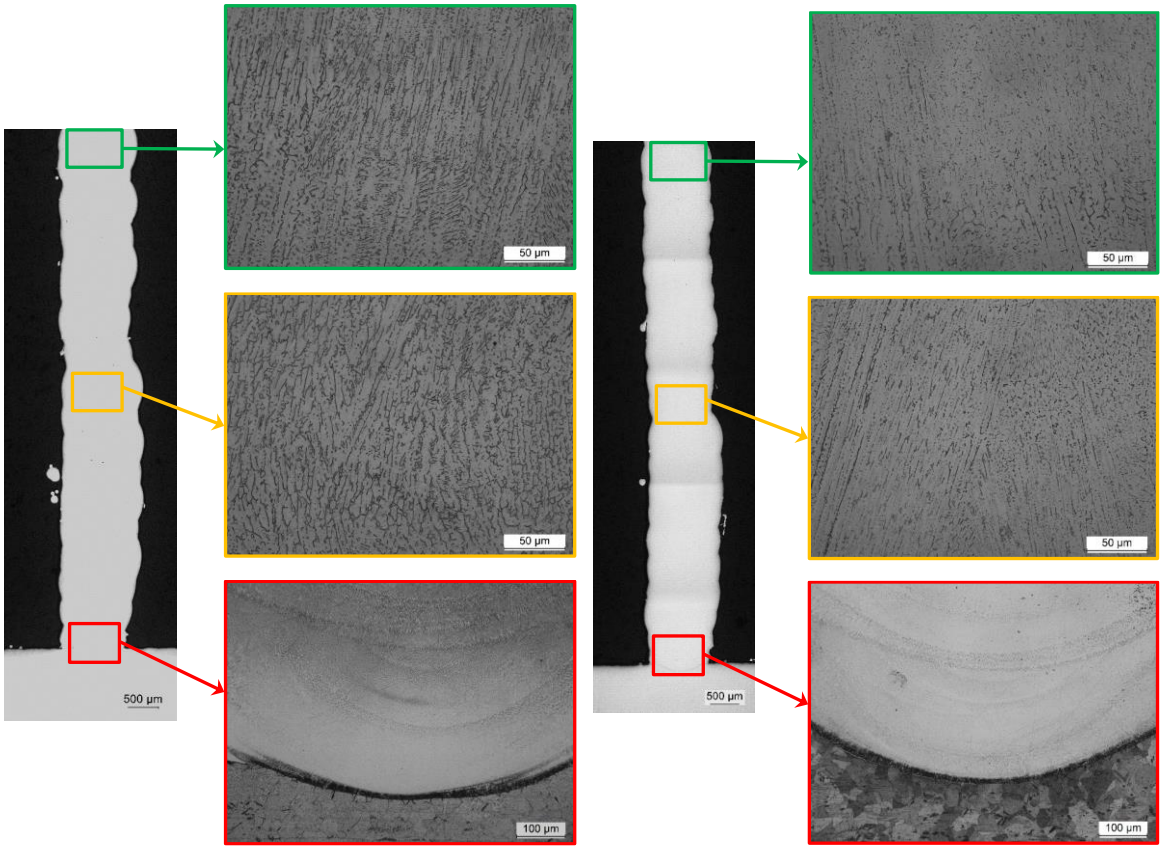

Figure 12. Photomicrographs by LOM of the walls made with SS316L. Sample 1 (e = 0.40, left) and Sample 2 (e = 0.04, right). Different study areas: Interface with the substrate (200X below), at 5 mm wall height (500X center) and 10 mm wall height (500X above).

For sample 3, the microstructures of the three areas under study (Figure 13) are different from those observed in the previous samples, since this material is a nickel-based and not an iron-based alloy. Three different zones are observed on the wall of sample 3. At the interface with the substrate, the dilution zone with the base material (AISI 304) and the good metallurgical bond between both can be clearly seen. In the micrograph of the middle zone of the wall, a columnar dendritic microstructure with epitaxial growth is already observed where changes in the direction of growth of the dendrites at the interface between strands are evident. In this middle zone the composition looks uniform without an apparent segregation. In this case, and according to literature [19,20], the microstructure is composed of a matrix of γ-Ni (light phase) and forming dendrites, small dark particles can be seen in globular and irregular forms that have precipitated along the interdendritic limits. An electron microscopy analysis at higher magnifications is necessary to visualize possible precipitation of hard phases such as the Laves phase and/or some other MC and TiN-type phases that are segregated during the rapid solidification process in this type of alloy.

Preprints (www.preprints.org) | NOT PEER-REVIEWED | Posted: 18 November 2020 doi:10.20944/preprints202011.0483.v1

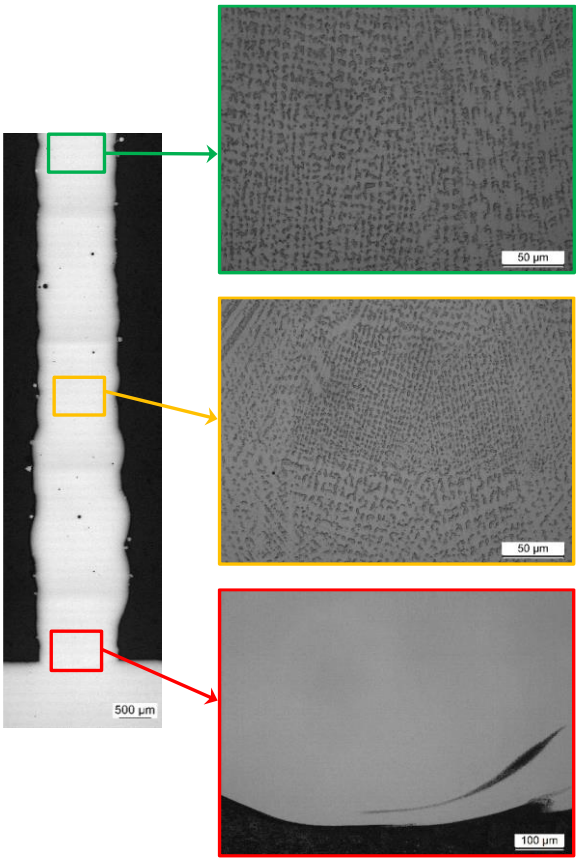

Figure 13. Photomicrographs by LOM of sample 3 (IN718, e = 0.40 and power control) in different areas. Interface with substrate (200X bottom), at 5 mm wall height (500X center) and 10 mm wall height (500X top).

It has been measured the microhardness (HV0.5 scale) of the deposited material, the dilution zone and the base metal. The graph in Figure 14 shows the microhardness profile obtained in samples 1 and 2 manufactured in SS 316L. As can be seen, there is a slight difference in the hardness along the wall. In the base metal (AISI 304) the hardness is about 198 HV, while in the dilution zone, there is a slight difference in chemical composition, since the substrate has a little less Cr but higher contents of Ni, C and Mo than the filler material. This makes that the resulting chemical composition in the first layer is a mixture of both, with a higher content of C and with the Mo as an alpha elements stabilizing the ferrite. The result is a slight increase in hardness. Additionally, the deposited material has a very fine dendritic microstructure, not at all comparable with the microstructure of a laminated material such as the base material. These walls were manufactured with variations in manufacturing process parameters every 10 layers (5 mm), decreasing the laser power by 50 W, in order to achieve stability in the growth of the wall and evaluate how these parameters influence the geometry, microstructure and hardness.

It is observed that in the first stretch of wall manufactured (Zone 1) for both walls a higher hardness value is obtained (230 HV) than in the second stretch manufactured with different parameters (214 HV). This behavior of the hardness is closely related to the microstructure and quantity of phases in each zone. As shown in Figure 14, in zone 1 the microstructure is finer than in zone 2 and perhaps the delta ferrite content in this zone is higher in zone 2.

Preprints (www.preprints.org) | NOT PEER-REVIEWED | Posted: 18 November 2020 doi:10.20944/preprints202011.0483.v1

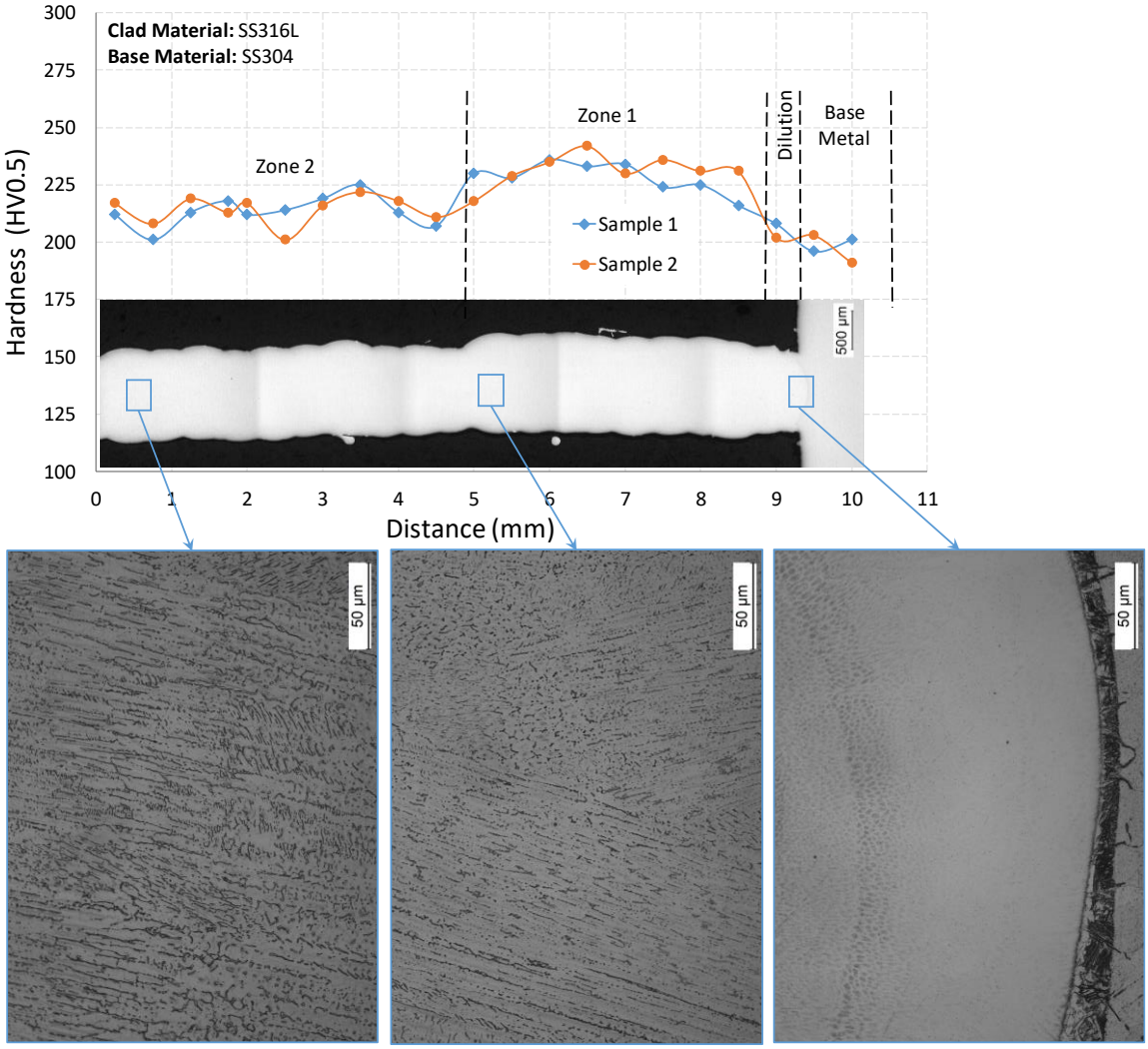

Figure 14. Microhardness profile on the walls made of SS316L (samples 1 and 2) and the microstructure in each area of the walls

In the case of the wall made with IN718 (sample 3), a laser power control system was used. This is a PID control system that acts by means of analogical signals in the laser beam source maintaining a set point of the size of the melt-pool and varying the laser power during the process. In this system the measurement of the size of the melt-pool is made by processing the image of the same obtained with a CCD camera installed in the optical head. In this case the wall thickness and the hardness of the material (see Figure 15) are more uniform than what was observed in samples 1 and 2.

Preprints (www.preprints.org) | NOT PEER-REVIEWED | Posted: 18 November 2020 doi:10.20944/preprints202011.0483.v1

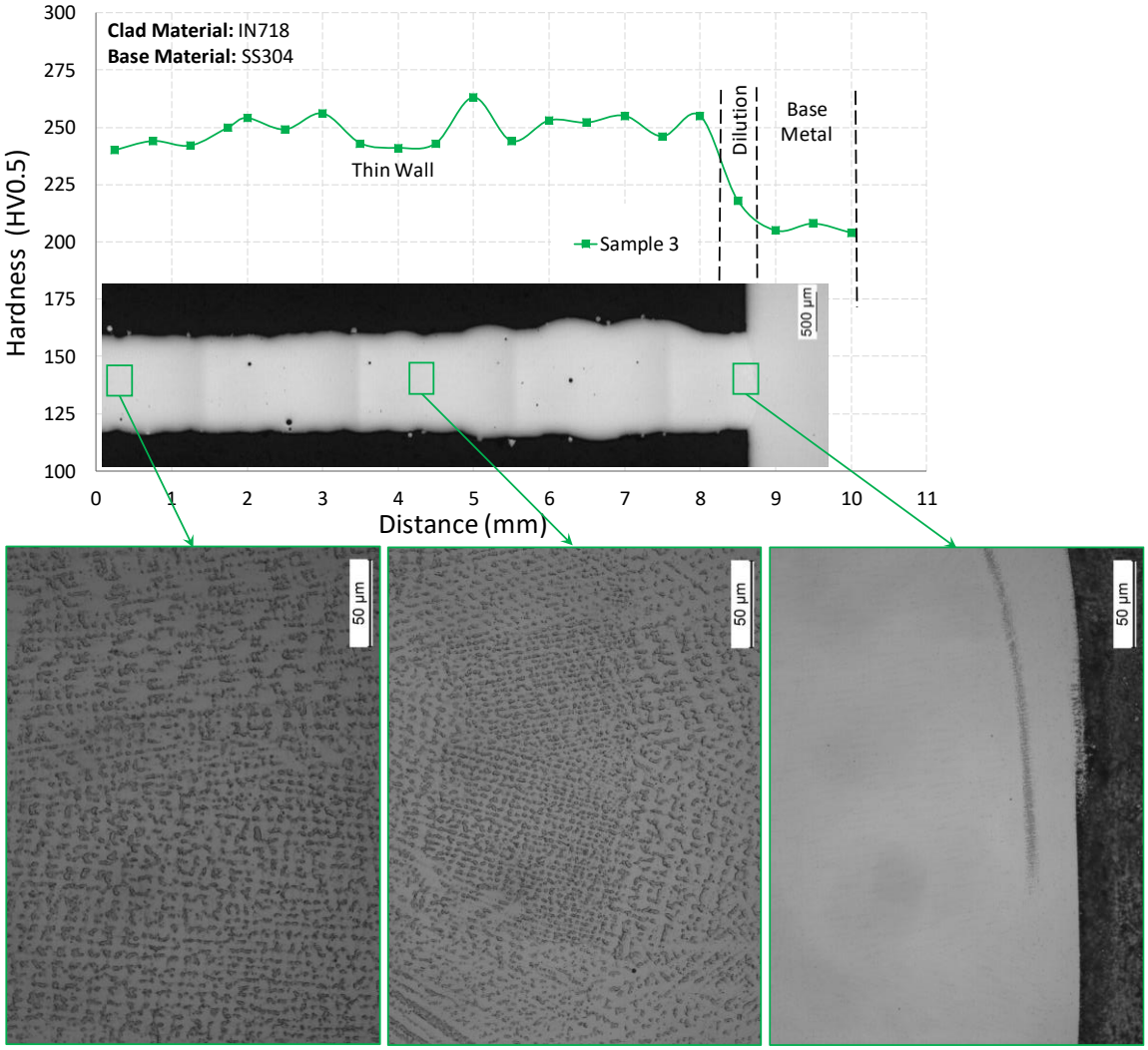

Figure 15. Microhardness profile on the wall manufactured with IN718 (sample 3) and the microstructure in each area of the wall.

The hardness values obtained and their hardness are compiled in Table 5. The improvement of the mechanical properties of the material in the wall manufactured by LMD is possible due to the adequate combination of process parameters and to the particular microstructure obtained in this type of process, as it has been shown here with the study of microstructure and its relationship with chemical composition and hardness.

Table 5. Average hardness values and deviation measured

Sample	Material	Hardness (HV0.5)			
		Base Metal	Dilution Zone	Wall	
				Zone 1	Zone 2
1	SS316L	198.5 ± 3.5	212.0 ± 5.7	230.0 ± 4.6	213.1 ± 5.8
2	SS316L	197.0 ± 8.5	216.5 ± 20.5	233.4 ± 4.6	214.2 ± 5.4
3	IN718	205.7 ± 2.1	239.7 ± 19.3	247.1 ± 6.7	

5. Conclusions

Based on the analysis made for the optimization of thin walls with sharp corners manufactured by LMD process with SS316L and IN718 alloys, the main conclusions are:

- It is possible to obtain thick walls (1 mm thickness) with only one bead/track per layer and straight/sharp corners at 90º after select the adequate process parameters and adjusting the precision of the kinematic on sudden changes in the direction of the deposition path.
- After adjusting the in-position parameter G502 for positioning precision on the FAGOR 8070 CNC station, it has been possible to obtain walls with minimal accumulation of material in the corner, and with practically constant layer thickness and height, with radii of internal curvature between 0.11 and 0.24 mm for two different precision at the straight corner of the wall and depending on the programmed speed.
- The best results have been obtained by identifying the correct balance between the percentage of decrease in programmed deposition speed and the precision in the positioning of the axes to reach the point defined as the corner (sudden change in the path direction) of the wall, with maximum speed reductions of 29% for a programmed speed of 20 mm/s and 61% for a speed of 40 mm/s.
- 3D analysis, acquisition and synchronization of the CNC kinematics data can be a platform for "digital twin" with data from both CNC and external process sensors, which is extremely valuable for manufacturing complex geometry parts with LMD.
- The manufactured walls show minimal defects such as residual porosities, and the microstructure and microhardness of the walls obtained has been analyzed..

Author Contributions: Conceptualization, Juan Carlos Pereira; Data curation, Herman Borokov and Josu Caminos; Formal analysis, Herman Borokov, Fidel Zubiri and Mari Carmen Guerra; Investigation, Fidel Zubiri; Methodology, Juan Carlos Pereira and Mari Carmen Guerra; Project administration, Juan Carlos Pereira; Writing – original draft, Juan Carlos Pereira; Writing – review & editing, Juan Carlos Pereira. All authors have read and agreed to the published version of the manuscript.

Funding: This work was partially supported by the Basque Government grant KK-2018/00004 (Departamento de Desarrollo Económico e Infraestructuras del Gobierno Vasco, Programa ELKARTEK Convocatoria 2018) through PROCODA project. And supported by the Ministry of Science and innovation of the Spain Government through the program "Ayudas destinadas a centros tecnológicos de excelencia CERVERA año 2019" from CDTI (Centro para el Desarrollo Tecnológico Industrial) in the frame of the CEFAM Project, grant CER-20191005.

Conflicts of Interest: The authors declare no conflict of interest. The funders had no role in the design of the study; in the collection, analyses, or interpretation of data; in the writing of the manuscript, or in the decision to publish the results.

References

1. International Organization for Standardization ISO/ASTM 52900:2015 Additive manufacturing — General principles — Terminology 2015.
2. ASTM International ASTM F3187-16, Standard Guide for Directed Energy Deposition of Metals 2016.
3. David Locke Laser metal deposition defined - TRUMPF Laser Technology Center. *Ind. Laser Solut. Manuf. Mag.* 2010.
4. Zhang, K.; Liu, W.; Shang, X. Research on the processing experiments of laser metal deposition shaping. *Opt. Laser Technol.* **2007**, *39*, 549–557, doi:10.1016/j.optlastec.2005.10.009.
5. Paulo Davim, J.; Oliveira, C.; Cardoso, A. Predicting the geometric form of clad in laser cladding by powder using multiple regression analysis (MRA). *Mater. Des.* **2008**, *29*, 554–557, doi:10.1016/j.matdes.2007.01.023.
6. Zhong, C.; Gasser, A.; Kittel, J.; Wissenbach, K.; Poprawe, R. Improvement of material performance of Inconel 718 formed by high deposition-rate laser metal deposition. *Mater. Des.* **2016**, *98*, 128–134, doi:10.1016/j.matdes.2016.03.006.
7. Woo, Y.-Y.; Han, S.-W.; Oh, I.-Y.; Moon, Y.-H.; Ha, W. Control of Directed Energy Deposition Process to Obtain Equal-Height Rectangular Corner. *Int. J. Precis. Eng. Manuf.* **2019**, *20*, 2129–2139, doi:10.1007/s12541-019-00226-6.

8. Baraldo, S.; Vandone, A.; Valente, A.; Carpanzano, E. Closed-Loop Control by Laser Power Modulation in Direct Energy Deposition Additive Manufacturing. In *Proceedings of 5th International Conference on the Industry 4.0 Model for Advanced Manufacturing*; Wang, L., Majstorovic, V. D., Mourtzis, D., Carpanzano, E., Moroni, G., Galantucci, L. M., Eds.; Springer International Publishing: Cham, 2020; pp. 129–143.
9. Bergs, T.; Kammann, S.; Fraga, G.; Riepe, J.; Arntz, K. Experimental investigations on the influence of temperature for Laser Metal Deposition with lateral Inconel 718 wire feeding. *Procedia CIRP* **2020**, *94*, 29–34, doi:https://doi.org/10.1016/j.procir.2020.09.007.
10. Tyralla, D.; Köhler, H.; Seefeld, T.; Thomy, C.; Narita, R. A multi-parameter control of track geometry and melt pool size for laser metal deposition. *Procedia CIRP* **2020**, *94*, 430–435, doi:https://doi.org/10.1016/j.procir.2020.09.159.
11. Garmendia, I.; Leunda, J.; Pujana, J.; Lamikiz, A. In-process height control during laser metal deposition based on structured light 3D scanning. *Procedia CIRP* **2018**, *68*, 375–380, doi:https://doi.org/10.1016/j.procir.2017.12.098.
12. Qiu, C.; Ravi, G. A.; Dance, C.; Ranson, A.; Dilworth, S.; Attallah, M. M. Fabrication of large Ti–6Al–4V structures by direct laser deposition. *J. Alloys Compd.* **2015**, *629*, 351–361, doi:https://doi.org/10.1016/j.jallcom.2014.12.234.
13. Möller, M.; Baramsky, N.; Ewald, A.; Emmelmann, C.; Schlattmann, J. Evolutionary-based Design and Control of Geometry Aims for AMD-manufacturing of Ti-6Al-4V Parts. *Phys. Procedia* **2016**, *83*, 733–742, doi:https://doi.org/10.1016/j.phpro.2016.08.075.
14. Zhu, G.; Li, D.; Zhang, A.; Pi, G.; Tang, Y. The influence of laser and powder defocusing characteristics on the surface quality in laser direct metal deposition. *Opt. Laser Technol.* **2012**, *44*, 349–356, doi:https://doi.org/10.1016/j.optlastec.2011.07.013.
15. Leitner, S.-H.; Mahnke, W. OPC UA--service-oriented architecture for industrial applications. *ABB Corp. Res. Cent.* **2006**, *48*, 61–66.
16. ASTM International ASTM E3-11(2017) Standard Guide for Preparation of Metallographic Specimens 2017.
17. ASTM International ASTM E407-07(2015)e1: Standard Practice for Microetching Metals and Alloys 2015.
18. Mukherjee, M. Effect of build geometry and orientation on microstructure and properties of additively manufactured 316L stainless steel by laser metal deposition. *Materialia* **2019**, *7*, 100359, doi:https://doi.org/10.1016/j.mtla.2019.100359.
19. Xin, B.; Ren, J.; Wang, X.; Zhu, L.; Gong, Y. Effect of Laser Remelting on Cladding Layer of Inconel 718 Superalloy Formed by Laser Metal Deposition. *Materials (Basel).* **2020**, *13*, 4927.
20. Jinoop, A. N.; Paul, C. P.; Mishra, S. K.; Bindra, K. S. Laser Additive Manufacturing using directed energy deposition of Inconel-718 wall structures with tailored characteristics. *Vacuum* **2019**, *166*, 270–278, doi:https://doi.org/10.1016/j.vacuum.2019.05.027.